Contactless Resistivity via an LC Oscillator

Daniel Weller

Advisor: Dr. Matthew Vannette, *SVSU Physics Department*

April 15, 2013

List of Figures

List of Tables

Abstract

An understanding of the magnetic response of materials as a function of frequency can provide information regarding the energy and time scales of different intra-material interactions. A convenient way to measure magnetic properties at radio frequencies (rf) is to measure frequency shifts in a self-resonant LC circuit. However, measurements of the rf magnetic properties of materials may be complicated by a convolution of the intrinsic magnetic response with a spurious electrical response associated with the normal state skin depth. Quantifying the effect of the skin depth contribution to the signal is the first step toward obtaining rf data that may be compared with data at lower frequencies where this convolution problem does not exist. We present the initial results of our efforts to disentangle these two contributions. By quantifying the geometric dependence of our measurement apparatus, we permit measurements of magnetic susceptibility in absolute units at radio frequency. This work forms the basis for all further studies of magnetic properties that make use of the self-resonant LC oscillator technique.

Introduction

The magnetic susceptibility, χ, of a material is related to its intrinsic electromagnetic properties. Magnetic susceptibility is a material dependent quantity that describes the magnetic behavior of an object in an applied magnetic field, H. The magnetic moments of an object experience an induced magnetization in response to the external magnetic field [1]. A material's magnetization relates to the strength of an applied magnetic field through χ

as

$$M = \chi H \tag{1}$$

In the above, H is the strength of the magnetic field in amperes per meter and M is magnetization in the same units. Magnetization varies among materials and is used to describe the density of magnetic moments which contribute to χ per unit volume [1]. Magnetic susceptibility is a dimensionless quantity and may be defined as $\chi = \frac{\mathrm{d}M}{\mathrm{d}H}$. The magnetic field within the material is the induction, B. The induction of a sample is the sum of the external field strength, H, and the magnetic field experienced due to the magnetization of moments within the sample [1].

$$B = H + 4\pi M \tag{2}$$

The sign of χ determines how the magnetic moments respond to an applied magnetic field [2]. In paramagnetic materials, $\chi > 0$, and the induced magnetization of the magnetic moments is in the same direction as H, strengthening the field within the material. In diamagnetic materials, $\chi < 0$, and the moments' magnetization opposes the magnetic field to weaken it in the material. All materials show some diamagnetic character due to a contribution from paired core electrons. However, this contribution is dominated by the paramagnetic component of χ in paramagnetic materials.

The electromagnetic properties of a material may be examined in an unconventional manner by use of a self-resonant LC oscillator. In an LC circuit, a capacitor (C) is coupled with an inductor (L). The capacitor is composed of two electrical conductors separated by an insulating, or dielectric, material [2]. When two conductors are isolated from one another, there will exist an

electric potential difference, V, between them. If the charge on one conductor is $+q$ and the charge on the other is $-q$, then a constant ratio $\frac{q}{V}$ will exist. This ratio is the capacitance, C.

$$C = \frac{q}{V} \tag{3}$$

This is only true for the $+q$,$-q$ charge configuration. A simple capacitor example is two parallel plates which store a charge q and are separated by air. For this case, capacitance may be defined based on geometry alone.

$$C = \frac{\varepsilon_0 A}{d} \tag{4}$$

The plate area is A, the separation distance between plates is d, and ε_0 is the electric permittivity of free space $\varepsilon_0 = 8.85 \times 10^{-12}$ Fm^{-1}.

If a capacitor has a potential difference, V, between its plates, an amount of work will be required to move charge $\mathrm{d}q > 0$ to the negative plate from the positive plate.

$$\mathrm{d}U = V\mathrm{d}q \tag{5}$$

This work is stored by the capacitor. The total energy stored by charging a capacitor with charge q is

$$\begin{aligned} \int_0^U \mathrm{d}U &= \int_0^q V\mathrm{d}q \\ &= \int_0^q \frac{q}{C}\mathrm{d}q \\ U_C &= \frac{q^2}{2C} \end{aligned} \tag{6}$$

The potential difference between the plates implies an electric field, and energy is stored within this electric field [2]. The capacitor's potential energy

reaches a maximum when the amount of charge stored is maximized. Once maximum charge is achieved, the capacitor discharges.

As the capacitor discharges in an LC circuit, charge flows through the inductor. An inductor is a coil of wire that induces a magnetic field when current, $i = \frac{\mathrm{d}q}{\mathrm{d}t}$, passes through it. The magnetic field, B, created by the current has a magnetic flux Φ_B related to the area A of the coil given by

$$\Phi_B = \int \vec{B} \cdot \mathrm{d}\vec{A} \tag{7}$$

This expression is true for one turn of the coil [2]. Since each turn has a flux, the total flux is

$$\Phi_{B,\,\mathrm{total}} = \sum_N \int \vec{B} \cdot \mathrm{d}\vec{A} \tag{8}$$

where N indexes the turns. As current in the inductor changes, so does the magnetic field. This varying magnetic field causes a change in Φ_B. By Faraday's Law of Induction, a potential difference is produced with the changing magnetic flux in the coil. This voltage V may be related to a change in flux by

$$\begin{aligned} V &= -\frac{\mathrm{d}\Phi_B}{\mathrm{d}t} \\ &= -\frac{\mathrm{d}\Phi_B}{\mathrm{d}i}\frac{\mathrm{d}i}{\mathrm{d}t} \end{aligned} \tag{9}$$

We now establish a definition for the inductance, L.

$$L = \frac{\mathrm{d}\Phi_B}{\mathrm{d}i} \tag{10}$$

From Eq. 10 we observe that a potential exists as the current changes with time in an inductor [2]. The inductance resists a change in current by changing the voltage to maintain constant current. The voltage in the inductor is

associated with magnetic field energy. The energy of the inductor's magnetic field is given by

$$\begin{aligned} \mathrm{d}U &= V\mathrm{d}q \\ &= \left(-L\frac{\mathrm{d}i}{\mathrm{d}t}\right)(i\mathrm{d}t) \\ \int_0^U \mathrm{d}U &= -\int_0^i Li\mathrm{di} \\ U &= -\frac{1}{2}Li^2 \\ U_L &= \frac{1}{2}Li^2 \end{aligned} \tag{11}$$

Again the energy of the system depends on the electric potential integrated with respect to the charge. The magnetic field energy is maximized when current is maximized in the inductor. This maximum occurs when no charge is stored on the capacitor. At this point all of the electric energy has transferred to magnetic field energy and the potential of the capacitor $V_C = 0$. Charge flows out of the inductor and the potential V_L changes to maintain a constant current through the inductor as stated earlier. The inductance recharges the capacitor to $-V_C$ where charge is stored on the opposite capacitor plate from where it started. The process continues in the opposite direction. According to the right hand convention, when the direction of the current changes, the direction of the magnetic field within the inductor changes as well. This changing direction creates an alternating magnetic field in the inductor.

Energy alternates between electric and magnetic forms in an LC circuit. The capacitor stores energy within an electrostatic field, whereas the inductor stores energy within an induced magnetic field. The total energy, U_T, at any time within the LC circuit is the sum of the electric field potential energy

and the magnetic field kinetic energy shown by

$$U_{\mathrm{T}} = U_C + U_L = \frac{1}{2}\frac{q^2}{C} + \frac{1}{2}Li^2 \tag{12}$$

The shifting between electric and magnetic field energy causes oscillations within the LC circuit [2].

We may draw an analogy to a mechanical oscillator where the total energy, U_{T}, is the sum of the potential and kinetic energies [2].

$$U_{\mathrm{T}} = \frac{1}{2}kx^2 + \frac{1}{2}mv^2 \tag{13}$$

In Eq. 13, k is a force constant, x is the displacement from equilibrium, m is the mass of the object, and v is the velocity of the object. The first term is the potential energy due to a restoring force, and the second term is the kinetic energy. When compared to Eq. 12, we notice that both total energy equations are a first order differential equation. The LC oscillator energy depends on q and the mechanical oscillator depends on x. The kinetic energy term for both equations involves the first derivative of these variables. For the LC oscillator, the current is $i = \frac{\mathrm{d}q}{\mathrm{d}t}$ and for the mechanical oscillator, the velocity is $v = \frac{\mathrm{d}x}{\mathrm{d}t}$. Hence, we see a close resemblance between the energy of an LC oscillator and a classical mechanical oscillator.

The oscillations occur at a particular frequency [2]. For a mechanical oscillator, the frequency of oscillation is

$$f = \frac{1}{2\pi}\sqrt{\frac{k}{m}} \tag{14}$$

Similarly, the LC oscillator operates at a resonant frequency given by

$$f = \frac{1}{2\pi}\sqrt{\frac{1}{LC}} \tag{15}$$

The frequency may be adjusted by changing either the inductance or the capacitance of the circuit. As an example of the range we work within, $f \approx 5.0$ MHz for $C = 100$ pF and $L = 10$ μH.

With a sample present in the inductor, the magnetic field within the region of space containing the sample is altered and the inductance of the apparatus changes accordingly. Consider a small change in $L \to L + \Delta L$. This will cause a change in $f \to f + \Delta f$. Eq. 15 implies

$$\begin{aligned} 2\pi(f + \Delta f) &= ((L + \Delta L)C)^{-\frac{1}{2}} \\ &= \left(LC\left(1 + \frac{\Delta L}{L}\right)\right)^{-\frac{1}{2}} \\ &= (LC)^{-\frac{1}{2}}\left(1 + \frac{\Delta L}{L}\right)^{-\frac{1}{2}} \end{aligned} \tag{16}$$

If $\frac{\Delta L}{L} << 1$ then a binomial expansion gives

$$2\pi(f + \Delta f) \approx (LC)^{-\frac{1}{2}}\left(1 - \frac{1}{2}\frac{\Delta L}{L}\right) \tag{17}$$

In this limit, we obtain a relationship between frequency shift and inductance change.

$$\begin{aligned} 2\pi f + 2\pi\Delta f &= (LC)^{-\frac{1}{2}} - (LC)^{-\frac{1}{2}}\frac{1}{2}\frac{\Delta L}{L} \\ \Delta f &= -\left(\frac{1}{2\pi(LC)^{\frac{1}{2}}}\right)\frac{1}{2}\frac{\Delta L}{L} \\ &= -f\frac{1}{2}\frac{\Delta L}{L} \\ \frac{\Delta f}{f} &= -\frac{1}{2}\frac{\Delta L}{L} \end{aligned} \tag{18}$$

The last of Eqs. 18 describes the resonant frequency shift, Δf, caused by inserting a metal sample into the inductor of an LC circuit [3]. In this experiment, metallic conductive samples were introduced into the inductor of the circuit causing a change in inductance ΔL. The base frequency is the resonant frequency of the empty coil.

From Eq. 2, we notice that the magnetic field within the metal sample is

$$B = H(1 + 4\pi\chi) \tag{19}$$

The magnetic susceptibility of the material alters the magnetic field within the inductor and causes a change in the coil inductance. It has been shown that χ is proportional to the inductance change ($\chi \propto \frac{\Delta L}{L}$) [4]. The frequency shift for a particular apparatus geometry relates to χ by

$$-4\pi\chi = G\frac{\Delta f}{f} \tag{20}$$

For diamagnetic samples, $\Delta f > 0$ and vice versa for paramagnetic materials. G is a coefficient that quantifies the relationship between χ and Δf and is based on geometrical aspects of the measurement apparatus. The geometric constant accounts for factors such as sample shape, effective sample radius, effective coil radius, and effective coil volume. For this work, it is important to note that G is assumed to be solely dependent on sample and coil geometry.

At low frequency, magnetic susceptibility has been measured in real units. This is relatively simple because at low frequency, susceptibility is dominated by only the effect of magnetic moments within the sample. However, at higher frequency, the material's electrical resistivity also contributes to χ. Electrical resistivity, ρ, is an intensive quantity that measures how strongly a material

resists an electric current [2]. Macroscopic resistance, R, is related to ρ and sample dimensions by

$$R = \frac{\rho l}{A} \tag{21}$$

where R is the resistance across the sample, l is the sample length parallel to current, and A is the cross-sectional area of the sample transverse to the current. Conventionally, resistivity is measured by a four-contact test. A current i is sent through a material with two wires and the voltage drop V across the sample is measured with another two wires. By utilizing Ohm's Law ($V = iR$) and Eq. 21 one can determine the resistivity of a material by measuring resistance for a sample of known dimensions.

Resistivity gives rise to a diamagnetic-like response that screens a time varying magnetic field from the interior of the material. This diamagnetic effect follows Lenz's Law, which states that induced eddy currents will form when a changing magnetic field interacts with a conducting material [2]. The electrons near the surface of the sample circulate in response to the varying magnetic field. Lenz's Law states that these currents will produce a magnetic field to oppose the change in the external magnetic field. This skin effect causes the magnetic field to penetrate only a finite distance into the sample [5]. In a normal conductor this penetration depth is known as the skin depth, δ. The skin depth is related to ρ and f by

$$\delta = \sqrt{\frac{\rho}{\pi \mu f}} \tag{22}$$

in Eq. 22, μ is the magnetic permeability. μ is described by

$$\mu = \mu_0 \mu_r \tag{23}$$

where μ_0 is the magnetic permeability of free space ($\mu_0 = 4\pi \times 10^{-7}$ H×m^{-1}) and μ_r is the relative permeability of the material [1]. For our samples $\mu_r = 1$ so $\mu = \mu_0$.

The skin effect influences the magnetic field within the coil and causes a change in inductance. From Eq. 22 it is apparent why the contribution from ρ only plays a role in susceptibility at higher frequency. In materials where δ is very large, the screening may be very weak. Conversely, when δ is small, the magnetic field no longer fully penetrates the material and the skin effect contributes to χ. The rf band is relatively unexplored for magnetic susceptibility studies due to the convolution of resistivity and a material's magnetic character.

Several universities and national labs are using a self-resonant LC oscillator technique to study χ through an observed frequency shift. Measurements of χ can be used to study magnetic phase transitions, long-range magnetic order, and superconductivity. Professor Agosta at Clark University uses this technique to study organic superconductors [6]. Dr. R. Gianetta at University of Illinois Urbana-Champaign has studied copper oxide superconductors [7] and iron compound superconductors are studied by R. Prozorov at Iowa State University with a self-resonant oscillator [8]. Many of these studies use a tunnel diode oscillator (TDO) or a CMOS oscillator circuit to measure frequency shift. The Lacerda group at the National High Magnetic Field lab in Los Alamos, New Mexico uses a TDO technique to make rf measurements [9]. The TDO has been established for quite some time. For example, in 1975, measured frequency shifts for a powdered sample of anhydrous $NiCl_2$ were related to inverse susceptibility to show that the sample exhibited Curie-Weiss behavior [10]. Field induced phase transitions have also been studied

by varying the strength of the external magnetic field. Pulsed magnetic field measurements have been made using this technique for certain organic compounds and conducting samples such as $Sr_3Ru_2O_7$ [11]. In these studies, χ is given in arbitrary units that relate χ to Δf through G.

This technique is commonly combined with a low-temperature cryostat to study magnetic phenomena at low temperatures. Many magnetic effects, such as phase transitions and hysteresis, are more significant at low temperature. As an example, this technique has been used to study the ferrimagnetic to paramagnetic phase transition in $TmCo_2$ occurring at about 4 K [12]. Many other experiments have studied the effect of temperature, magnetic field, and frequency noise for this technique with these types of LC oscillators [3][13]. Therefore, this technique can be an accurate method for detecting magnetic phenomenon in many different samples.

This oscillator technique has a high geometric dependence. In a study done by the Lacerda group, frequency shift of uranium nickel metal compounds are measured and used to calculate the material's resistivity [9]. Fig.

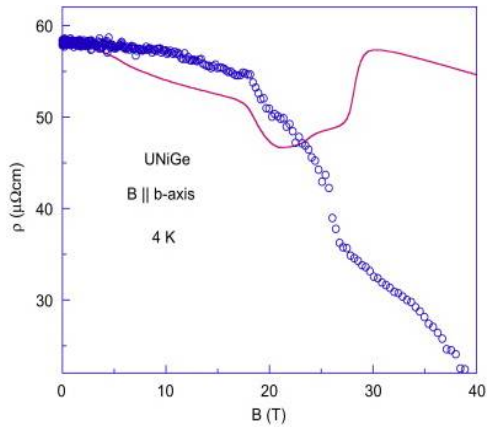

Figure 1: UNiGe plot of ρ vs. magnetic field B at 4 K from Lacerda *et al.* [9] showing measured ρ values from a four-probe test (open circles) and calculated ρ data from frequency shift (solid line).

1 shows a plot from this study displaying measured resistivity data and calculated resistivity data from frequency shift measurements. Open circles show measured data for resistivity and the solid line shows calculated resistivity data from measured frequency shifts. Clearly, the measured ρ data disagrees with the data calculated from experimental frequency shifts. These disagreements are attributed to geometrical factors [9] although this neglects the possibility of magnetic effects. Therefore, in order to determine χ in absolute units at radio frequency, for a particular apparatus G must be quantified.

Resistivity's contribution to χ derives from the skin effect for different materials. Prozorov *et al.* [14] have shown for superconductors shaped into rectangular slabs that χ relates to δ by

$$-4\pi\chi = \frac{1}{1-N}\left[1 - \frac{\lambda}{R}\tanh\left(\frac{R}{\lambda}\right)\right] \tag{24}$$

where N is the demagnetization factor, λ is the London penetration depth, and R is a characteristic length. A similar relationship has been established for normal conducting metals [15].

$$-4\pi\chi = \frac{1}{1-N}\left[1 - \frac{\mu\delta}{2R}\tanh\left(\frac{2R}{\delta}\right)\right] \tag{25}$$

where R is a characteristic dimension based on sample geometry, μ is magnetic permeability, and δ is the skin depth. Skin depth for conductors has a similar role in its relationship to χ as λ does for superconductors. For the samples we are using, we assume $N = 0$, and for a particular sample shape and size in a given coil, G and R are constants. Hence, through their

relationships to χ we can relate G to δ and R by

$$G\frac{\Delta f}{f_0} = \left[1 - \frac{\mu\delta}{2R}\tanh\left(\frac{2R}{\delta}\right)\right] \tag{26}$$

The resonant frequency of the circuit with an empty coil is f_0. The skin depth contribution to χ is measurable when δ is very small compared R. In the $\delta << 2R$ limit, the hyperbolic tangent saturates to one. It follows that

$$\begin{aligned} G\frac{\Delta f}{f_0} &= 1 - \frac{\mu\delta}{2R} \\ &= 1 - \frac{1}{2R}\sqrt{\frac{\mu\rho}{\pi f_0}} \\ \frac{1}{2R}\sqrt{\frac{\mu\rho}{\pi f_0}} &= 1 - G\frac{\Delta f}{f_0} \\ \sqrt{\mu\rho} &= 2R\sqrt{\pi f_0} - 2RG\sqrt{\pi}\frac{\Delta f}{\sqrt{f_0}} \\ \sqrt{\mu\rho} &= a\sqrt{f_0} - b\frac{\Delta f}{\sqrt{f_0}} \end{aligned} \tag{27}$$

where $a = 2R\sqrt{\pi}$ and $b = 2RG\sqrt{\pi}$. This implies

$$\frac{b}{a} = G \tag{28}$$

Inserting a metallic sample induces a change in the resonant frequency provided $\Delta f << f_0$. At a given base frequency, resistivity may be connected to a frequency shift from the sample's presence in the inductor. This provides a noncontact way of determining resistivity based only on the inductance change associated with inserting the sample into the coil. Upon rearrangement, the last of Eqs. 27 becomes

$$\frac{\Delta f}{\sqrt{f_0}} = \frac{a}{b}\sqrt{f_0} - \frac{\sqrt{\rho}}{b} \tag{29}$$

If Δf for a given sample and coil is measured at several f_0, a plot of $\frac{\Delta f}{\sqrt{f_0}}$ versus $\sqrt{f_0}$ is expected to be linear with slope $\frac{a}{b} = \frac{1}{G}$ and y-intercept $\frac{-1}{b}\sqrt{\rho}$. This provides a method for determining G for a particular sample shape and coil. In the experiment outlined in this thesis, G is determined as a first step in obtaining χ in absolute units at high frequency. Here we demonstrate how to determine the geometric dependence of a particular experimental apparatus. We will be working within the rf band ($f \approx 6 - 17$ MHz) to quantify resistivity's contribution to several metals' magnetic susceptibilities.

Experimental

A Colpitts LC oscillator is used to measure the frequency shift associated with the presence of a metal sample in the inductor. Fig. 2 shows the diagram for our measurement circuit with circuit component values included. Sample and apparatus geometry relate susceptibility to an observed change

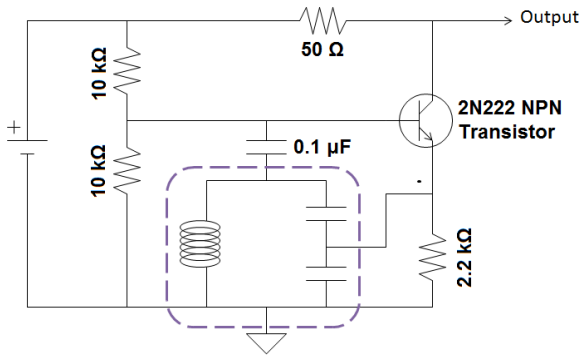

Figure 2: Colpitts oscillator circuit diagram showing arrangement of circuit components, component values, transistor label, and LC oscillator outlined by the dashed line.

in resonant frequency. The inductor coil is shown in Fig. 3. The coil is made of copper wire (38 AWG) wound around a nonmagnetic plastic straw and has $N \approx 27$ turns, a radius of $r \approx 3.5$ mm, and a length of $\ell \approx 1.6$ cm. This

same coil was used for all frequency shift measurements.

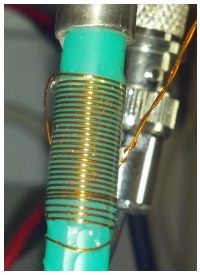

Figure 3: Inductor coil used in LC oscillator.

Frequency shifts were measured at five different base frequencies. Resonant frequencies were adjusted by changing the capacitors on the circuit. Table 1 shows the nominal capacitances for each run and their associated base frequencies. Base frequencies were measured for the empty coil each

Capacitance (pF)	235	82.5	50	32	23.5
f_0 (MHz)	6.32856	10.4070	12.5372	15.2788	16.5932

Table 1: Capacitance values and associated resonant frequencies.

time before and after the samples were inserted.

The sample holder used for mounting samples in the inductor is depicted in Fig. 4. The sample holder was made of a sapphire rod connected to a

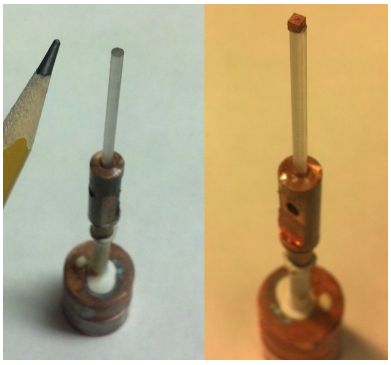

Figure 4: Empty sample holder with pencil for scale and sample holder with Cu sample mounted.

copper block and ceramic rod. It was constructed using nonmagnetic materials so as to not affect the magnetic field within the inductor. Samples were mounted to the tip of the sample holder with high vacuum grease. The sample holder extended just short of the center of the coil so that the sample was as near the center of the coil as possible when present in the apparatus. This point in the coil stayed fixed for each sample. Therefore, each sample was at the same location in the coil for every data run.

Metallic samples with nonmagnetic signature were used to study the resistivity's contribution to susceptibility. Samples of copper (Cu), aluminum (Al), zinc (Zn), tin (Sn), and lead (Pb) of purity 99.9-99.989 % were shaped into rectangular solids. Impurities could potentially contribute to magnetic signatures of metal samples, but for our samples this effect is negligible. The samples were shaped using 600 and 800 grit sandpaper to polish them to a size of about 1.5 mm on each edge. For instance, our Cu sample had dimensions of $1.409\text{mm}^3 \times 1.469\text{mm}^3 \times 1.490\text{mm}^3$. In Fig. 5, photographs of the samples are shown next to a millimeter scale.

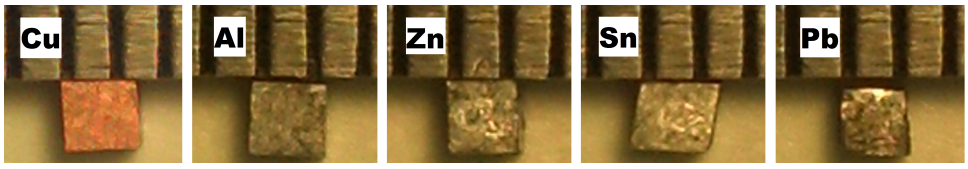

Figure 5: Random sample faces of Cu, Al, Zn, Sn, and Pb.

For the first set of runs, the samples were randomly placed on the sample holder without regard to their orientation with respect to the coil axis. Frequency shifts for these nonoriented samples were measured at each base frequency. Care was not given to how samples were placed on the holder in order to determine the effect of sample orientation on results. A second set of data runs was performed. This time the orientation of each sample was

maintained for all base frequencies. The sides of the designated upward faces were marked with a pencil and oriented in the same direction perpendicular to the coil axis for every run. Fig. 6 shows the same samples side by side with the marked faces shown. Assuming that the coil is perfectly cylindrical,

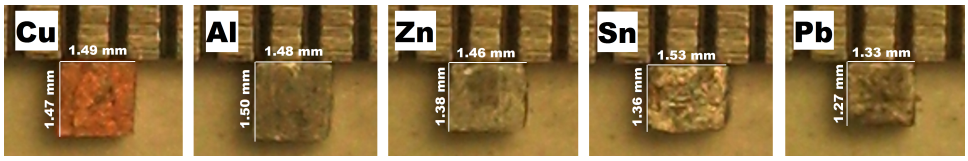

Figure 6: Samples of Cu, Al, Zn, Sn, and Pb showing faces oriented perpendicular to coil axis for second set of data runs.

it should not make a difference which direction each side face is directed. This ensured that the orientation of each sample was constant for all data runs. Length measurements of the faces perpendicular to the coil axis are also shown in Fig. 6. All measurements were conducted at room temperature and resistivity values for each material were taken from literature [5].

Data & Analysis

We may estimate the self-inductance of our coil by starting with Eq. 15 and obtaining an equation in the form of a line which relates $\frac{1}{C}$ at several values to $4\pi^2 f^2$ by

$$\frac{1}{C} = 4\pi^2 f^2 L \tag{30}$$

By plotting $\frac{1}{C}$ as a function of $4\pi^2 f^2$, we obtain a line with a slope of L shown in Fig. 7. This slope displays a value of $L = 4\ \mu$H for the inductance of our coil. This can be compared to a formula for L in an infinite solenoid

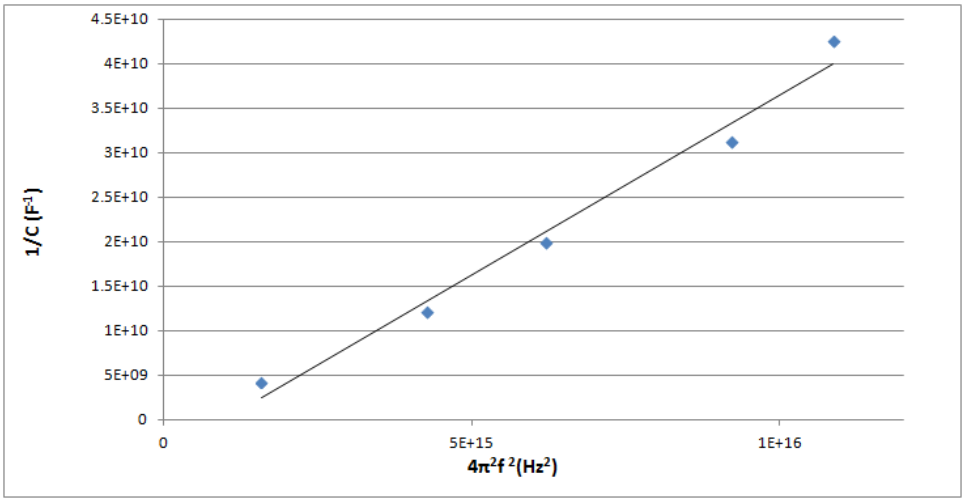

Figure 7: Plot showing data points and linear best fit for $\frac{1}{C}$ vs. $4\pi^2 f^2$ with slope $L = 4\ \mu$H.

with a uniform magnetic field [2].

$$L = \frac{\mu_0 \pi r^2 N^2}{\ell} \tag{31}$$

In the above, r is the coil radius, N is the number of turns in the coil, and ℓ is the coil length. We find that for our particular coil

$$\begin{aligned} L &= \frac{(4\pi \times 10^{-7}\text{Hm}^{-1})(\pi(0.0035\text{m})^2)27^2}{0.016\text{m}} \\ L &= 2.20 \times 10^{-6}\text{H} \end{aligned} \tag{32}$$

Although there is a significant difference ($\approx 45\%$) between our calculated and experimental inductance, our coil is behaving on the order of magnitude that we would expect for its size when compared to theoretical values. By using the same coil and sample holder for each run, the geometric dependence of our apparatus is limited to only the geometry of our samples.

Frequency shift data was collected for randomly oriented samples first at the five base frequencies. This data is plotted in Fig. 8. Regression values

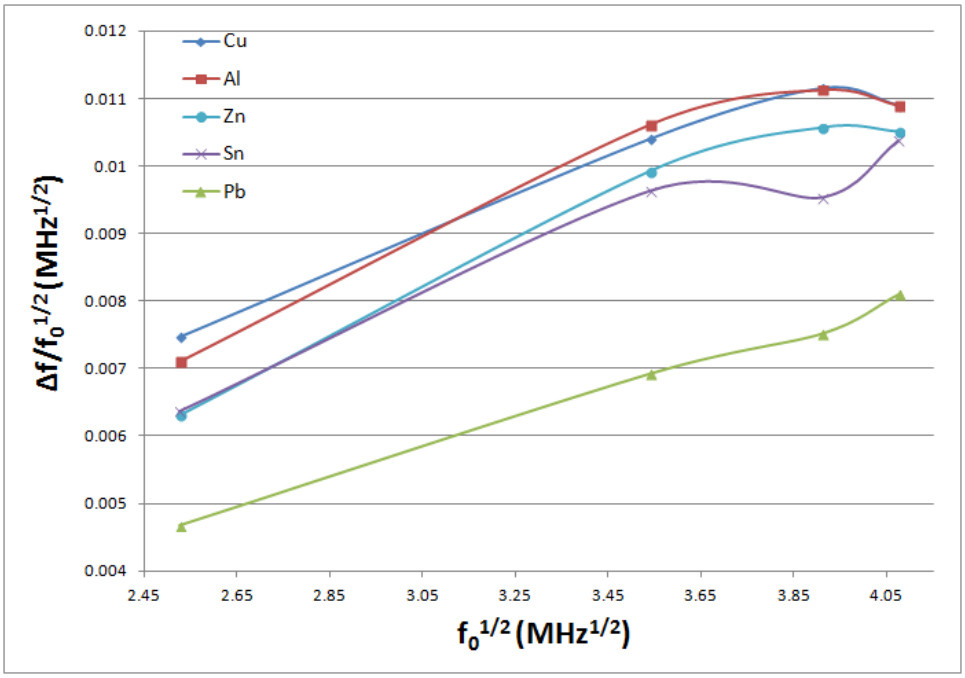

Figure 8: Five plots of $\Delta f/\sqrt{f_0}$ vs. $\sqrt{f_0}$ for randomly oriented samples with lines serving as guides to the eye.

for the linear fits of these data range from $R^2 = 0.93$ to $R^2 = 0.96$. The data closely follows a linear trend and supports the model for frequency shifts at different base frequencies from Eq. 29. Smooth lines were added as guides to the eye to illustrate inconsistencies of measured frequency shifts. For example, Pb very closely follows the predicted linear trend, but Sn follows a more random curved path. These findings can be explained by inspection of the nonuniformly oriented samples in Fig. 5. Pb has a square face with perpendicular adjacent faces extending directly downward. Sn clearly has a parallelogram for a face and the top is offset from the bottom. This irregularity in shape leads to a different dependence of Δf due to the orientation of our Sn sample when in the inductor. The orientation effect manifests in the data by the "hook" at higher frequencies in Fig. 8.

In an attempt to eliminate the nonlinearity, a second set of data runs was

performed. This time frequency shift data was taken for each sample oriented in the same direction in the inductor. Frequency shifts for oriented samples at each base frequency are shown in Table 5 located in the Appendix Section at the end of the report. The data from Table 5 is plotted on a common set of axes $\Delta f/\sqrt{f_0}$ vs. $\sqrt{f_0}$ in Fig. 9. Regression analysis shows that all

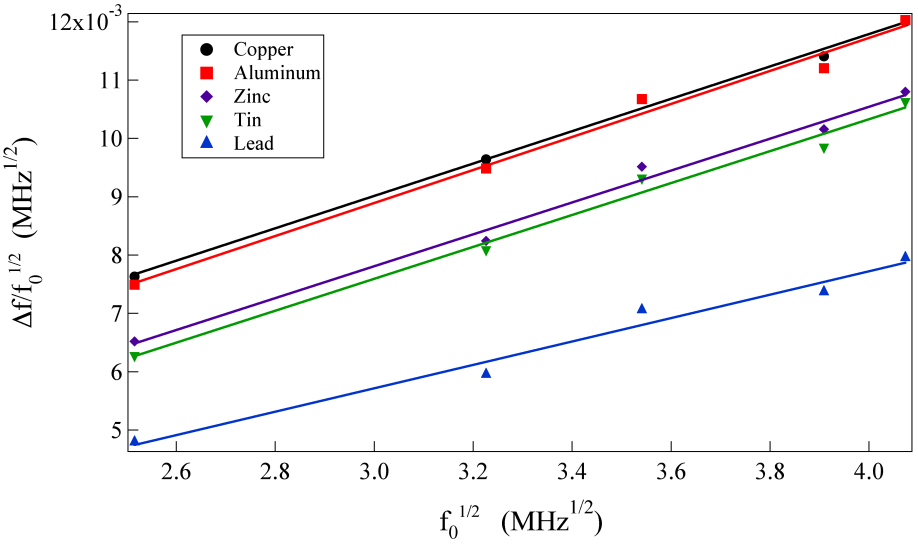

Figure 9: Five linear trends for $\Delta f/\sqrt{f_0}$ vs. $\sqrt{f_0}$ with consistently oriented samples.

of the plots strongly support a linear model ($R^2 = 0.98$ to $R^2 = 0.99$). This data suggests that sample orientation can significantly affect the inductance change when using this technique.

Resistivity values were not calculated for this data. Literature values of ρ for the five metal samples at 295 K are shown in Table 2 [5]. The linear fits for

Sample	Cu	Al	Zn	Sn	Pb
Resistivity ($\mu\Omega$ cm)	1.71	2.69	6.01	11.74	20.76

Table 2: Resistivity values for five metals at 295 K.

each sample in Fig. 9 are ordered from top to bottom by increasing resistivity

as we would expect. This is noticeable in the y-intercepts of Fig. 9. Pb has the highest resistivity by far and has the lowest intercept, whereas Cu has the lowest resistivity and the highest intercept. These findings are supportive of this technique as a method for determining a material's resistivity.

Nevertheless, there could be several factors contributing to error in ρ when considering the y-intercept of these plots. Below $f < 6$ MHz in the rf band, our signal becomes too unstable for accurate measurement. We expect that all y-intercepts would be negative due to positive resistivity and b values. Stray capacitances play a larger role in signal noise at lower frequencies. However, Cu and Al have positive y-intercepts implying a negative value for ρ or b. These disagreements can be explained by the flatness of the slope in our data. If the slope varies by a small amount, the y-intercept can be dramatically altered. This means that any small change in measured frequency can have a large effect on the y-intercept. Due to our frequency noise the lowest base frequency is significantly far from the y-axis, and data closer to the intercept becomes difficult to accurately measure. With a more stable oscillator, data at lower frequency could accurately be obtained, allowing for an accurate determination of ρ.

Each of the data series clearly shows a linear trend allowing determination of G. Geometric coefficient values determined by fits from Eq. 29 are given for our five samples in Table 3. The variation in G is quite small if we neglect

Sample	Cu	Al	Zn	Sn	Pb
G value	360.4	353.1	365.6	365.7	498.4

Table 3: G values for samples shown in Fig. 6.

Pb. There is about 3 % difference between these samples indicating that G

is reasonably robust. However, the geometric coefficient is quite different for the Pb sample. This is likely to be attributed to different sample size. From Fig. 5, one can visibly observe a lack of shape and size regularity between samples. As shown in Fig. 6, our sample edges range from roughly 1.3 mm to 1.5 mm. Volumes for each sample were calculated and are shown in Table 4. The Cu sample is quite large and the Pb sample is comparatively

Sample	Cu	Al	Zn	Sn	Pb
Volume (mm^3)	3.085	2.989	2.997	2.726	2.312

Table 4: Volumes for five metal samples.

small. A difference in 0.2 mm can lead to a severe difference in sample volume when operating at this size level. In comparing the Cu and Pb samples, the sample volume differs by approximately 25 % which can have a significant effect on the inductance change. These volume differences play a significant role in the outcome of Δf. However, the Sn sample has a volume that differs by approximately 10 % from Zn, yet its G value is the same ($G \approx 366$). The difference in shape between the Zn and Sn samples

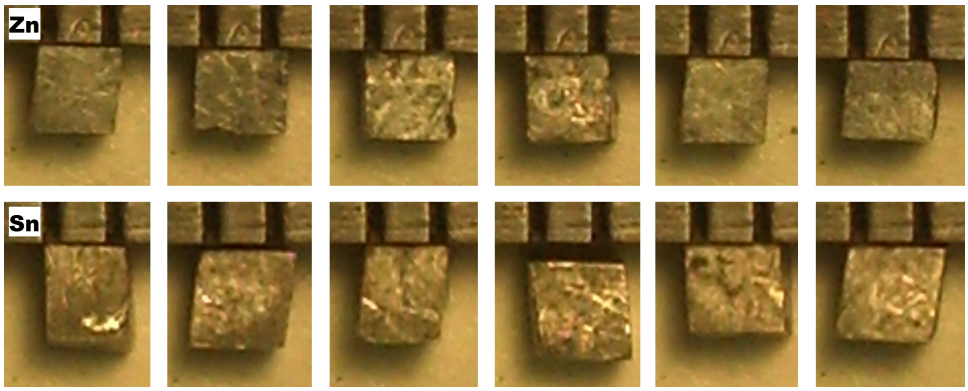

Figure 10: Two six panel figures of Zn (top) and Sn (bottom) illustrating difference in sample shape.

is apparent upon inspection of Fig. 10. Not only does the sample size

contribute to G but also the sample shape can have a significant effect by changing the angle at which the sample interacts with the magnetic field. It seems that the difference in shape offsets the volume discrepancy in G for our Sn sample. The samples' orientation with respect to the coil axis greatly influences observed frequency shifts. This different shape between samples is most visibly noticeable in the Sn, Cu, and Pb samples. The Sn sample is a rhomboid, Cu is a large rectangular prism, and Pb is a small cube. In addition, at such a small size, samples become difficult to handle. Dents and bevels can occur simply through handling samples with tweezers and may contribute to sample deformities. This data suggests an extremely low tolerance for variation in sample size and geometry when using this technique to determine ρ.

Conclusion

An LC oscillator may be used as a contactless measurement device for determining the material properties of a sample. In particular, this experiment placed normal metallic conductive samples into the coil of the oscillator. The sample's resistivity contributes to χ at radio frequency and affects the frequency shift associated with the metal sample's presence. This experiment quantifies G to extend the foundation of this technique for studies regarding the electrical and magnetic properties of materials. By quantifying G, susceptibility values may be determined in absolute units at higher frequencies. This work allows further experiments to be done regarding electromagnetic phenomena occurring in the rf band.

To extend this experiment, samples that exhibit magnetic signatures may be studied at higher frequency. By quantifying the resistivity's contribution

to χ, the contribution from the magnetic moments within the sample can be analyzed. Additionally, this technique may be extended to study insulating samples where ρ is very large. This increased ρ causes δ to also increase. For these samples, the resistivity does not contribute to χ, but χ is still related to a frequency shift for a particular apparatus as in Eq. 20. The observed frequency change quantifies χ for insulating samples at radio frequency with this technique. These results may be compared to those obtained at lower frequencies.

LC oscillator measurements are being performed by several laboratories around the world, yet none of these large laboratories have quantified G for their apparatus. They simply study χ in arbitrary units of Δf or f. Although these units allow qualitative detection of magnetic phenomena, obtaining susceptibility in absolute units lets researchers compare results from material studies between different labs. This is an important step in developing the self-resonant oscillator technique as a robust and useful method for material property measurement. Our determination of the geometric dependence of this type of apparatus validates the experiments going on in these laboratories and provides a framework for further study using this technique.

Appendix

Sample	f_0 (MHz)	$\sqrt{f_0}$ ($\sqrt{\text{MHz}}$)	Δf (MHz)
Cu	6.32858	2.516	0.0192
	10.4070	3.226	0.0311
	12.5373	3.541	0.0378
	15.2788	3.909	0.0446
	16.5932	4.073	0.0489
Al	6.32858	2.516	0.0189
	10.4070	3.226	0.0306
	12.5373	3.541	0.0379
	15.2788	3.909	0.0438
	16.5932	4.073	0.0490
Zn	6.32858	2.516	0.0164
	10.4070	3.226	0.0266
	12.5373	3.541	0.0337
	15.2788	3.909	0.0397
	16.5932	4.073	0.0440
Sn	6.32858	2.516	0.0158
	10.4070	3.226	0.0261
	12.5373	3.541	0.0330
	15.2788	3.909	0.0385
	16.5932	4.073	0.0433
Pb	6.32858	2.516	0.0118
	10.4070	3.226	0.0192
	12.5373	3.541	0.0250
	15.2788	3.909	0.0288
	16.5932	4.073	0.0324

Table 5: Frequency shift values for samples at five different base frequencies.

Bibliography

[1] Wangsness, *Electromagnetic Fields* (John Wiley & Sons, Hoboken, New Jersey, 1986) p. 328.

[2] Halliday, Resnick, Walker, *Fundamentals of Physics* (John Wiley & Sons, Hoboken, New Jersey, 2008) p. 826.

[3] H. Srikanth, J. Wiggins, H. Rees, Rev. Sci. Instrum. **70**, 3097 (1999).

[4] R. B. Clover, W. P. Wolf, Rev. Sci. Instrum. **41**, 617 (1970).

[5] N. W. Ashcroft, N. D. Mermin, *Solid State Physics* (Thomson Learning, Toronto, Ontario, 1976) p. 8.

[6] William A. Coniglio, Laurel E. Winter, Kyuil Cho, C. C. Agosta, B. Fravel, L. K. Montgomery, Phys. Rev. B **83**, 224507 (2011).

[7] R. Prozorov, D. D. Lawrie, I. Hetel, P. Fournier, R.W. Giannetta, Phys. Rev. Lett. **93**, 147001 (2004).

[8] K. Cho, H. Kim, M. A. Tanatar, J. Hu, B. Qian, Z. Q. Mao, R. Prozorov, Phys. Rev. Lett. **93**, 147001 (2004).

[9] A. M. Alsmadi, S. Alyones, C. H. Mielke, R. D. McDonald, V. Zapf, M. M. Altarawneh, A. Lacerda, S. Chang, S. Adak, K. Kothapalli, H. Nakotte, J. Mag. and Mag. Materials **321**, 3712 (2009).

[10] F. Habbal, G. E. Watson, P. R. Elliston, Rev. Sci. Instrum. **46**, 192 (1975).

[11] E. Ohmichi, E. Komatsu, T. Osada, Rev. Sci. Instrum. **75**, 2094 (2004).

[12] A. I. Figueroa, J. Bartolomé, J. M. García del Pozo, A. Arauzo, E. Guerrero, P. Téllez, F. Bartolomé, L. M García, J. Mag. and Mag. Materials **324**, 2669 (2012).

[13] C. T. Van Degrift, Rev. Sci. Instrum. **46**, 599 (1974).

[14] R. Prozorov, R. W. Giannetta, A. Carrington, F. M. Araujo-Moreira, Phys. Rev. B **62**, 115 (2000).

[15] R. Prozorov, M. D. Vannette, G. D. Samolyuk, S. A. Law, S. L. Bud'ko, P. C. Canfield, Phys. Rev. B **75**, 14413 (2007).